

Zinc oxide nanowires and nanorods fabricated by vapour-phase transport at low temperature

Xu, Chunxiang; Sun, Xiaowei; Dong, Zhili; Yu, M. B.; My, T. D.; Zhang, X. H.; Chua, S. J.; White, Timothy John

2004

Xu, C., Sun, X., Dong, Z. L., Yu, M. B., My, T. D., Zhang, X. H., et al. (2004). Zinc Oxide Nanowires and Nanorods Fabricated by Vapour-Phase Transport at Low Temperature. *Nanotechnology*, 15(7).

<https://hdl.handle.net/10356/95569>

<https://doi.org/10.1088/0957-4484/15/7/022>

© 2004 Institute of Physics Publishing. This is the author created version of a work that has been peer reviewed and accepted for publication by Nanotechnology, Institute of Physics Publishing. It incorporates referee's comments but changes resulting from the publishing process, such as copyediting, structural formatting, may not be reflected in this document. The published version is available at: <http://dx.doi.org/10.1088/0957-4484/15/7/022>.

Downloaded on 20 Mar 2024 16:29:09 SGT

Zinc oxide nanowires and nanorods fabricated by vapour-phase transport at low temperature

*C X Xu¹, X W Sun^{1,5}, Z L Dong², M B Yu³, T D My³, X H Zhang⁴, S J Chua⁴
and T J White²*

¹ *School of Electric and Electronic Engineering, Nanyang Technological University, Nanyang Avenue, 639798, Singapore*

² *Institute of Environmental Science and Engineering, Nanyang Technological University, 18 Nanyang Drive, 637723, Singapore*

³ *Institute of Microelectronics, 11 Science Park Road, Singapore Science Park II, 117684, Singapore*

⁴ *Institute of Materials Research Engineering, 3 Research link, 117602, Singapore*

⁵ *Author to whom any correspondence should be addressed.*

E-mail: exwsun@ntu.edu.sg

Abstract

Using zinc chloride as source material, zinc oxide nanowires and nanorods were fabricated by a vapour-phase transport method at low temperature. The nanowires grown on gold-coated silicon showed a uniform diameter of about 40 nm, and the nanorods on copper-coated silicon grew upwards to form flower-like arrays. The x-ray diffraction and transmission electron microscopy analyses demonstrated that the nanostructural zinc oxide grew along the [0001] direction. The growth process was attributed to a vapour–liquid–solid mechanism. Distinct photoluminescent behaviours were observed for zinc oxide nanostructures grown on gold-coated and copper-coated silicon wafers.

1. Introduction

With a wide direct band gap (3.4 eV), a strong excitonic binding energy (60 meV) and an oxygen vacancy modulated conduction mechanism, zinc oxide (ZnO) has attracted remarkable attention in optoelectronics and sensor areas [1]. Recently, the demonstrations of room temperature ultraviolet lasers [2–4], field effect transistors [5, 6] and field emission arrays [7–10] based on ZnO nanowires have stimulated great interest in developing functional nanodevices. As a simple method, vapour-phase transport (VPT) [2–13] has been employed to fabricate various nanostructures of ZnO. However, the synthesis temperature in general VPT process is usually near to or even higher than 1000 °C. For example, Yang's group synthesized ZnO nanowires at about 800–925 °C [2, 12]; Pan *et al* [13] fabricated ZnO nanoribbons at 1400 °C; and our group

prepared nanopins at 1150 °C [9]. The temperature is too high for fabricating nanostructural ZnO on low temperature substrates, such as glass. However, it is very desirable to synthesize nano-ZnO at low growth temperature for device application. In order to reduce the fabrication temperature, chemicals with low melting point, such as metal zinc [14] and zinc acetylacetonate [15], have been utilized as source materials, and various techniques such as metal–organic vapour-phase epitaxy (MOVPE) [16] and hydrothermal decomposition [17] have also been used.

Zinc halide should be a good candidate for use in low temperature fabrication of ZnO because of its low melting point; however, it is rarely used, although one paper [18] reported the fabrication of ZnO nanobelts employing zinc chloride (ZnCl_2) as source material on an alumina plate at 700 °C. In this paper, we shall report on ZnO nanowires and nanorod arrays fabricated on various substrates by thermally evaporating and oxidizing the ZnCl_2 powders at 350–500 °C, by a method based on the VPT process.

2. Experiment

The fabrication of ZnO nanostructures was carried out in a two-layer quartz tube by vapour-phase transport. The raw material used was ZnCl_2 powder, which was placed in a concavity of the inner slender quartz tube. Gold- and copper-coated silicon slices were put downstream at the opening of the inner slender quartz tube, which was also in the constant temperature zone of the tube furnace. The temperature of the substrates was set to 500 °C. The temperature of the source region was 350 °C due to the temperature gradient. It is worth pointing out that, in our process, the source has a lower temperature compared to the substrate. Nitrogen gas with a flow rate of 100 sccm was used as the carrier gas to carry the vapours generated downstream to the substrate. And oxygen gas with a flow rate of 20 sccm was introduced into the quartz tube from a separate inlet to oxidize the vapour of ZnCl_2 . A grey layer of product covered the surface of the substrate surface after 30 min reaction.

To characterize the crystal properties and analyse the growth process, scanning electron microscopy (SEM) was employed to examine the morphology of the product. The crystal structure of the samples was characterized by x-ray diffraction (XRD) using copper $\text{K}\alpha_1$ radiation. A JEOL 3010 high resolution transmission electron microscope (HRTEM) operated at 300 kV was employed to detect the lattice structure. Photoluminescence (PL) was also utilized to characterize the emission spectra of ZnO samples excited by the 350 nm wavelength from a Xe lamp. The 350 nm excitation light with a bandwidth of 2 nm was filtered with a grating. The Raman scattering spectra were measured by a Renishaw Ramanscope under the excitation of an argon laser operating at 514.5 nm. All measurements were taken at room temperature.

3. Results and discussion

Figure 1 shows the XRD patterns of the product grown on Au-coated and Cu-coated silicon substrates, respectively. It can be seen that all the diffraction peaks match with the standard database of hexagonal structural ZnO although the relative intensity differs between the two samples. This indicates that both samples are composed of wurtzite structural ZnO with the lattice constants of $a = 0.3250$ nm and $c = 0.5207$ nm.

Figure 2 shows the SEM image of ZnO nanowires fabricated on an Au-coated silicon substrate. It can be seen from figure 2 that the substrate is covered with a layer of short rods with

diameters of several hundred nanometres. The nanowires lie on the nanorod layer. Figure 2 shows that the nanowires have uniform diameter of about 40 nm. Their lengths are several tens of microns. Figure 3 shows the nanorod array grown on Cu-coated Si wafer. The nanorods tend to grow upwards to form flower-like radial arrays. It can be seen from the enlarged SEM images of figures 3(b) and (c) that the nanorods are 200–500 nm in diameter and about 10 μm in length, and they have hexagonal cross-sections with sharp tips.

The growth process of the catalyst-assisted nanostructural crystals follows the vapour–liquid–solid (VLS) mechanism [2] in general. With a temperature of 350 $^{\circ}\text{C}$, ZnCl_2 powder at the source region was evaporated and carried into the higher temperature region. On the substrate surface, the vapour reacted with metallic catalyst and condensed into liquid zinc–catalyst alloy nanodroplets. Each droplet acted as a nucleus that is energetically favoured to adsorb incoming zinc vapour and further influence the morphology of the ZnO nanostructures. When the droplets became supersaturated, the metallic zinc recombined with oxygen to form ZnO nanocrystals and further grow epitaxially into nanorods and nanowires. Figures 4(a) and (b) show the TEM images of an individual ZnO nanowire grown on Au-coated Si with low and high magnification respectively. A ripple-like contrast observed in figure 4(a) is due to strain resulting from the bending of the nanowire [13]. Figure 4(b) clearly presents the lattice structure of the ZnO nanowire. It is noted that the d -space between adjacent planes is 0.26 nm, which matches that of adjacent (0002) planes of wurtzite structural ZnO. The rectangle inserted in figure 4(b) shows a unit cell of ZnO with oxygen and zinc atoms indicated. The lattice structure demonstrates that the nanowire grew along [0001] orientation. The layer of short nanorods formed (figure 2) before the nanowire is probably due to the higher vapour pressure and the rapid growth in the early stage.

The sharpened hexagonal nanorods grown on Cu-coated Si substrate should have a similar growth process to those on Au-coated Si substrate. A hexagonal and prismatic nucleus has been achieved in our previous report [19]. According to Laudise's argument [20] on polar crystal growth, the formation of the hexagonal shape and the prismatic tops of ZnO nanorods is attributed to the different growth rates for different crystal faces. To obtain the lowest formation energy, the fastest growth velocity must be along the [0001] direction [21]. The crystal facet with faster growth velocity tends to disappear and the facet with slower growth velocity is prone to remain. Therefore sharp tips are formed during the nanorod growth.

Figure 5 shows normalized PL spectra of the samples. Both of the samples illustrate a stronger UV emission band peaked at 380 nm and a weaker green band peaked at 515 nm. It has been demonstrated that the UV emission is originated from the band edge excitonic recombination [22] and the green emission is attributable to the electron transfer from the singly ionized oxygen vacancy state to the photoexcited hole in the valence band [23]. For the ZnO sample fabricated on Au-catalysed substrate, the PL spectrum emits mainly UV light, as shown in figure 5. Although the nanorods fabricated on Cu-catalysed substrate also radiate strong UV emission, the green light is much stronger than that for nanorods on the Au-catalysed substrate. This indicates that more defects exist in the nanorod array fabricated on Cu-coated silicon wafer. The inset in figure 5 shows the normalized XRD peaks corresponding to (0002) lattice plane. It can be seen that the full width at half-maximum of the peak from Au-catalysed ZnO is a bit narrower than that from the Cu-catalysed sample. This demonstrates the better crystal quality of the former. Two optical modes have been observed in Raman spectra of ZnO samples, as shown in figure 6. The strong Raman shift peak at 437 cm^{-1} originates from the nonpolar optical phonon

E_2 mode, which is a typical Raman active branch of hexagonal ZnO [24]. The weak peaks at 584 cm^{-1} correspond to the $E_1(\text{LO})$ mode, which is caused by the formation of oxygen vacancies and zinc interstitials in ZnO [24]. The strong E_2 peak and the hardly observed $E_1(\text{LO})$ peak demonstrate that Au-catalysed ZnO has a typical hexagonal structure and better crystal quality. The weak $E_1(\text{LO})$ peak that appeared in the Raman spectrum of the Cu-catalysed ZnO nanorods indicates the defects existing in the sample. The measurement results for both XRD and Raman scattering are consistent with the PL behaviours.

4. Conclusion

Using zinc chloride powders as source materials, ZnO nanowires and nanorod arrays were fabricated on Au-coated and Cu-coated silicon wafers at low temperature. The nanostructural ZnO grew along the [0001] orientation. The growth process was attributed to a VLS mechanism. The different defect concentration is responsible for the relative intensity of the green emission observed for Au- and Cu-catalysed samples. The low temperature growth process is beneficial for further preparation of nanodevices with low cost.

Acknowledgements

Sponsorship from Research Grant Manpower Fund (RG51/01) of Nanyang Technological University and Nippon Sheet Glass Foundation is gratefully acknowledged.

References

- [1] Sun X W and Kwok H S 1999 *J. Appl. Phys.* **86** 408
- [2] Huang M, Mao S, Feick H, Yan H, Wu Y, Kind H, Weber E, Russo R and Yang P 2001 *Science* **292** 1897
- [3] Johnson J, Yan H, Schaller R, Haber L, Saykally R and Yang P 2001 *J. Phys. Chem. B* **105** 11387
- [4] Sun X W, Yu S F, Xu C X, Yuen C, Chen B J and Li S 2003 *Japan. J. Appl. Phys.* **42** L1229
- [5] Kind H, Yan H, Messer B, Law M and Yang P 2002 *Adv. Mater.* **14** 158
- [6] Arnold M S, Avouris P, Pan Z W and Wang Z L 2003 *J. Phys. Chem. B* **107** 659
- [7] Lee C J, Lee T J, Lyu S C, Zhang Y, Ruh H and Lee H J 2002 *Appl. Phys. Lett.* **81** 3648
- [8] Zhu Y W, Zhang H Z, Sun X C, Feng S Q, Xu J, Zhou Q, Xiang B, Wang R M and Yu D P 2003 *Appl. Phys. Lett.* **83** 144
- [9] Xu C X and Sun X W 2003 *Appl. Phys. Lett.* **83** 3806
- [10] Xu C X, Sun X W, Chen B J, Shum P, Li S and Hu X 2004 *J. Appl. Phys.* **95** 661
- [11] Xu C X, Sun X W and Chen B J 2004 *Appl. Phys. Lett.* **84** 1540
- [12] Yang P, Yan H, Mao S, Russo R, Johnson J, Saykally R, Morris N, Pham J, He R and Choi H J 2002 *Adv. Funct. Mater.* **12** 323
- [13] Pan Z W, Dai Z R and Wang Z L 2001 *Science* **291** 1947
- [14] Lyu S C, Zhang Y, Lee C J, Ruh H and Lee H J 2003 *Chem. Mater.* **15** 3294
- [15] Wu J J and Liu S C 2002 *Adv. Mater.* **14** 215
- [16] Park W I, Kim D H, Jung S W and Yi G C 2002 *Appl. Phys. Lett.* **80** 4323
- [17] Vayssieres L, Keis K, Hagfeldt A and Lindquist S E 2002 *Chem. Mater.* **13** 4365
- [18] Zhang J, Yu W and Zhang L 2002 *Phys. Lett. A* **299** 276
- [19] Xu C X and Sun X W 2003 *Japan. J. Appl. Phys.* **42** 4949

- [20] Laudise R A and Ballman A A 1960 *J. Phys. Chem.* **64** 688
- [21] Li W J, Shi E W, Zhong W Z and Yin Z W 1999 *J. Cryst. Growth* **203** 186
- [22] Haupt M, Ladenburger A, Sauer R, Thonke K, Glass R, Roos W, Spatz J P, Rauscher H, Riethmuller S and Moller M 2003 *J. Appl. Phys.* **93** 6525
- [23] Vanheusden K, Wareen W L, Seager C H, Tallant D R, Voigt J A and Gnade R F 1996 *J. Appl. Phys.* **70** 7983
- [24] Xu C, Xu G, Liu Y and Wang G 2002 *Solid State Commun.* **122** 175

List of Figures

- Figure 1 The XRD pattern of nanostructural ZnO fabricated on (a) Au-coated and (b) Cu-coated Si substrates.
- Figure 2 An SEM image of ZnO nanowires fabricated on Au-coated Si wafer.
- Figure 3 SEM images of ZnO nanorod arrays fabricated on Cu-coated Si wafer with (a) low, (b) moderate and (c) high magnifications.
- Figure 4 TEM images of an individual ZnO nanowire grown on Au-coated Si with low (a) and high (b) resolution.
(This figure is in colour only in the electronic version)
- Figure 5 Normalized PL spectra of nanostructural ZnO fabricated on Au-coated and Cu-coated Si substrates. The inset shows the XRD peak of (0002)
- Figure 6 Raman scattering spectra of nanostructural ZnO fabricated on Au-coated and Cu-coated Si substrates.

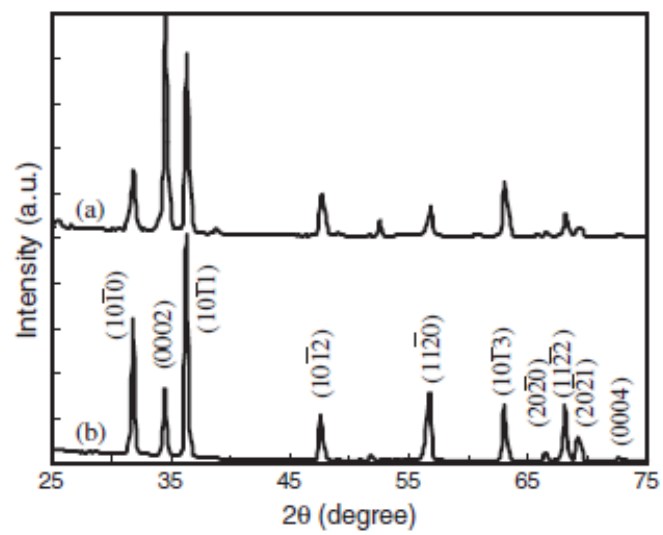


Figure 1

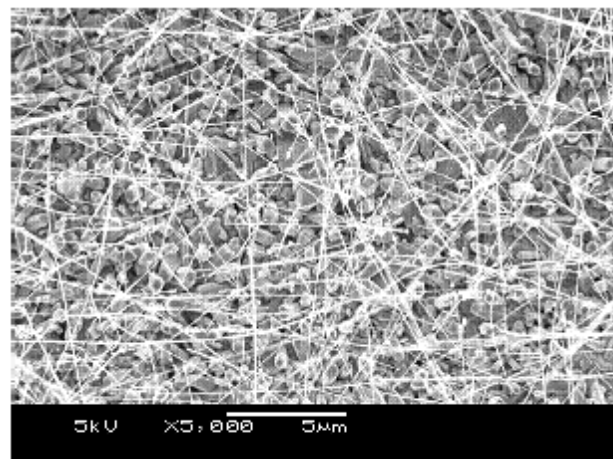


Figure 2

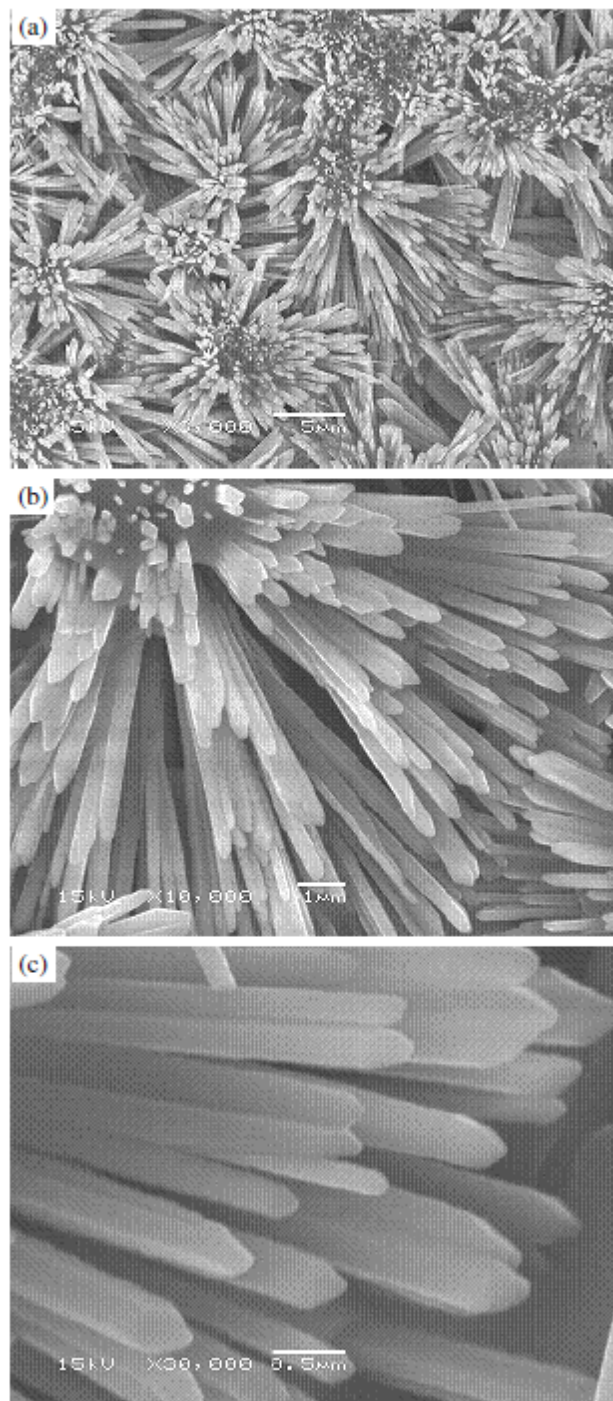


Figure 3

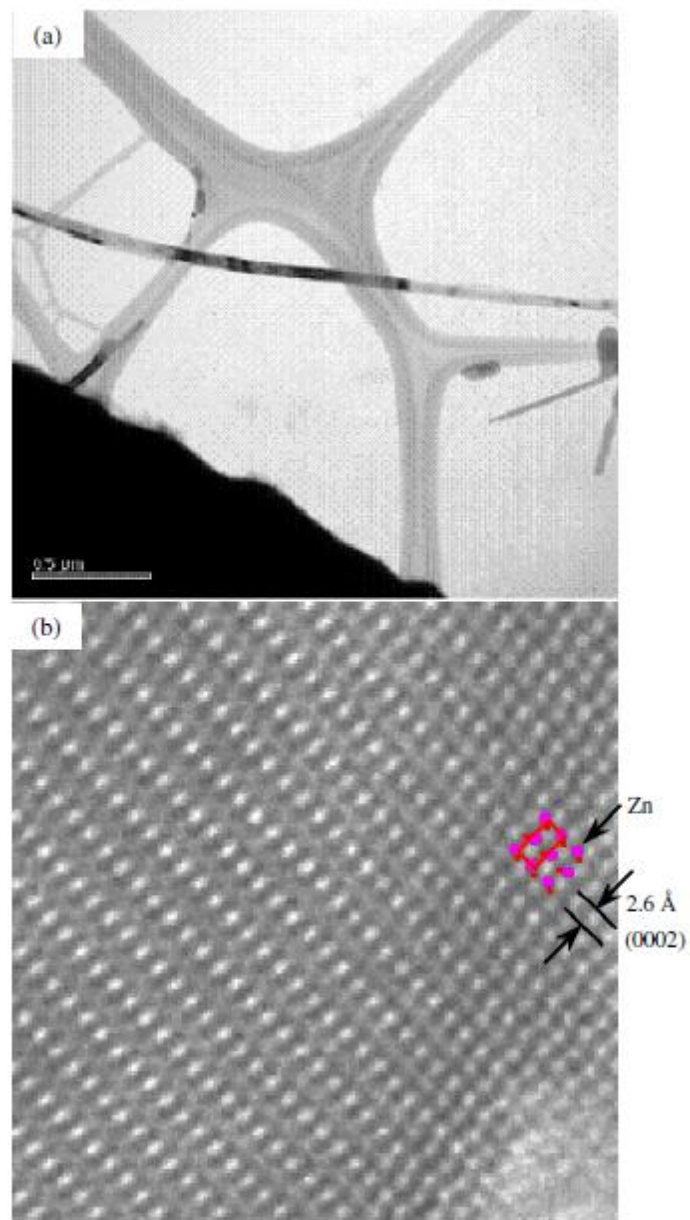


Figure 4

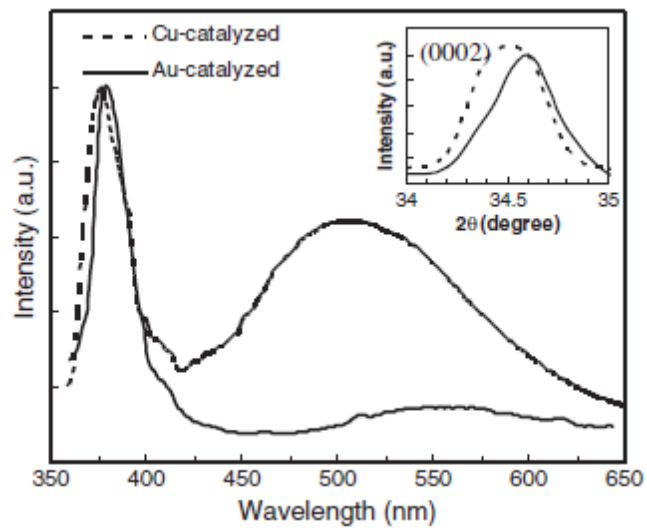


Figure 5

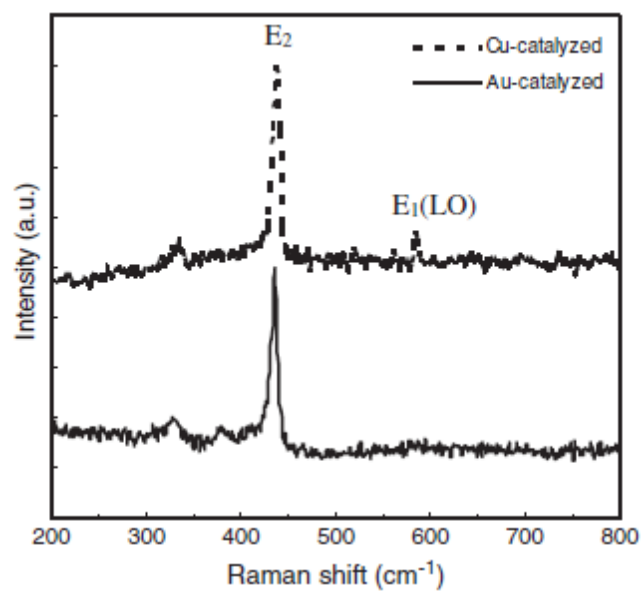


Figure 6